# CHAPTER- V

# THE ELECTROCHROMIC PROPERTIES OF NIOBIUM OXIDE THIN FILMS

# CHAPTER-V

# THE ELECTROCHROMIC PROPERTIES OF NIOBIUM OXIDE ($Nb_2O_5$) THIN FILMS

## 5.1 Introduction

Intercalation compounds can be formed through the uptake or exchange of guest molecules, atoms, or ions by host lattices having suitable structures. These processes are well known examples of solid-state reactions that can occur at low temperatures. The books edited by Mandel Corn [1] and by Whittingham and Jacobson [2] may serve as standard texts for intercalation phenomena. The hosts can be of different types, including framework lattices and layer structures. The guest species can also show a large variety, but the types of interest for electrochromism are almost exclusively $H^+$ (protons) and the alkali ions $Li^+$, $Na^+$, $K^+$ etc. These mobile ions can be co-ordinated to water molecules. Among the possible reaction mechanisms, the partinent one for electrochromism are related to host lattices with some electronic conductivity, for which an effective lattice charge can be accomplished by the intercalation. Thus the intercalation proceeds under synchronous uptake of ions and electrons into the solid. From a chemical point of view, the intercalation process can be considered as a topotactic redox reaction by electron and ion transfer [3]. The reaction is reversible, and the host lattice retains its basic structural integrity during the course of forward and backward reaction. Anion intercalation is unfavorable under most conditions, which can be understood from steric and energetic arguments [4].

In cyclic voltammetry, a voltage is applied between the niobium oxide film and a counter electrode. The voltage is swept back and forth between two set points, usually in a triangular manner, alternatively, the voltage is pulsed between two

levels. The current flowing into and out of the film in conjunction with the ion intercalation/deintercalation is measured. Cyclic voltammetry can be used non-quantitatively to give a 'fingerprint' of the electrochemical processes, to trace reversible and irreversible effects, and to ascertain voltage levels that yield stable operation. Voltages outside the stability range can lead to gas evolution, metal electroplating , etc. Quantitative cyclic voltammetry is also possible [5], for example for measurements of charge densities associated with intercalation/ deintercalation processes. Commercial potentiostats can be used for cyclic voltammetry, an alternative low-cost system particularly suitable for electrochromics was described recently by Kirkup et al. [6].

Niobium oxide has been studied extensively due to its broad industrial applications especially in opto-electronic technology [7-11]. Niobium oxide film is a promising counter electrode material in electrochromic devices. Niobia has excellent chemical stability and corrosion resistance in both acid and base media, which makes it useful in a wide range of electrochromic devices. The relationship between microscopic and macroscopic properties, and deposition parameters provides important guidance when optimizing material characteristics for a given application. This is especially true for oxides of niobium, since niobium oxide films exhibit different electrical and optical properties depending on deposition techniques and fabrication parameters [8].

Electrochromism is a phenomenon related to a persistent and reversible optical change induced electrochemically, whose macroscopic effect is a change in

colour [12]. A niobium oxide film shows a transparent to brownish gray or blue electrochromism with ion injection. The quality of an EC material is measured by its colouration efficiency, which is its transmittance contrast between coloured and bleached states relative to injected charge, response time, and chemical stability. These properties depend on the materials properties of the $Nb_2O_5$ films. The best EC properties are observed in porous amorphous niobium oxide films made by sputtering [13]. There are some studies on EC properties of $Nb_2O_5$ films fabricated by, electron beam evaporation [14], plasma oxidation [15], chemical vapour deposition [18], metallo-organic chemical vapor deposition [16], and sol-gel process [17]. Conventional techniques such as evaporation and sputtering need capital intensive and complicated equipment.

Very few studies have been reported on the electrochromic properties of $Nb_2O_5$. Reichmann and Bard [18] and Gomes et al. [19] found a blue colouration in opaque $Nb_2O_5$ grown thermally at 500°C on niobium metallic disk, Alves [20] has confirmed the possibility to insert $Li^+$ ions in a $Nb_2O_5$ ceramic prepared from a commercial powder sintered at ~ 800°C. Ohtani et al. [21] have reported the preparation of $Nb_2O_5$ films exhibiting good electrochromic properties by using sol-prepared from Nb ethoxide. $Nb_2O_5$ coatings appear therefore promising candidates for their use in various solid-state electrochemical devices such as photovoltaic solar cells [22] and electrochromic devices [23]. One fundamental characteristic of this oxide film is its rapid and reversible coloration when small ions such as $H^+$ or $Li^+$ are inserted in the layer lattice. The optical transmission of

the coating changes typically from a quasi-transparent state (T ~ 85%) to less than T ~ 20% in a large optical range from the near UV to near IR. It exhibits either a blue colour when the coating is crystallized or a gray colour when it is amorphous.

## 5.2 Experimental

$Nb_2O_5$ thin films were prepared by spray pyrolysis technique. Standard niobium solution was prepared as described in chapter III, Section 3.3.3 and was used as a precursor solution. $Nb_2O_5$ thin films were deposited onto fluorine doped tin oxide (F.T.O) coated glass substrates maintained at various temperatures from 250 to 450°C in the interval of 50°C. These samples were annealed at 500°C for four hours in air, which then used as working electrode in a three electrode EC cell. Graphite was a counter electrode and 0.1 N $H_2SO_4$ was an electrolyte. The voltages were measured with respect to the standard calomel electrode (SCE).

Cyclic voltammetry (CV) was carried out using scanning potentiostat EG and G model PAR-362 and X-Y (t) recorder. For CV , a cyclic potential sweep is imposed on an electrode and the current response was observed at different scan rates. Stability of $Nb_2O_5$ films in 0.1N $H_2SO_4$ was tested by repeating CV for several times. Chronoamperometry (CA) studies were carried out using X-Y (t) recorder in conjunction with scanning potentiostat and the variation of colouration and bleaching current with respect to time at fixed potential was recorded. Optical transmittance spectra of coloured and bleached films, in the range 350 to 850 nm wavelength , were recorded by using Hitachi-330 spectrophotometer.

## 5.3 Results and discussion

This chapter is devoted to electrochemical measurements of $Nb_2O_5$ thin films and testing of electrochromism in these films. This has been done by employing electrochemical characterization techniques such as cyclic voltammetry, chronoamperometry and spectrophotometric measurements.

During rudimentary experiments it was found that all the un-annealed samples (N250 to N450) get dissolved in 0.1N $H_2SO_4$ electrolyte. Therefore electrochemical measurements of the un-annealed samples were not possible. However, annealed samples (NA250 to NA 450) were quiet adherent and withstood electrochemical characterizations for prolonged period. Therefore these samples were subjected to the characterizations without further problems.

### 5.3.1 Electrochemical characterisation

#### 5.3.1.1 Cyclic voltammetry (CV)

If the potential of an electrode in the electrochemical cell is controlled externally, the solution can be made to 'adjust' by electron transfer to approach equilibrium with the electrode potential. In many electrochemical experiments, the solution initially has only form of a redox couple present and the electrode is initially set at a potential such that this form does not undergo electron transfer. This insures that the experiment begins at zero faradaic current. The electrode potential is then to a position that favours electron transfer. The manner in which the potential is changed gives rise to a profusion of electrochemical controlled potential techniques.

CV is a potential controlled 'reversal' electrochemical experiment. A cyclic potential sweep is imposed on electrode and current response is observed. Analysis of the current response can give information of the thermodynamics and kinetics of electron transfer at the electrode-solution interface, as well as the kinetics and mechanisms of solution chemical reactions initiated by the heterogeneous electron transfer.

Fig. 5.1 shows the overall view of the CV experiment. A potentiostat system sets the control parameters of the experiment. Its purpose is to impose on an electrode (the working electrode) a cyclic linear potential sweep and to output the resulting current-potential curve. This sweep is described in general by its initial (Ei), switching (Es), final (Ef) potentials, and sweep (or scan) rate. The potential as a function of time is;

$$E = Ei + Vt \quad \text{(forward sweep)} \qquad .....(5.1)$$

$$E = Es - Vt \quad \text{(reverse sweep)} \qquad .....(5.2)$$

More complicated sweeps are possible, such as the option of a second potential. Multiple cycles are sometimes used, but in many instances these will not be more informative than a single cycle. However, the electrochromic stability of an EC electrode in an electrolyte can be studied by repeating these cycles several times. The term 'linear sweep voltammetry' (LSV) is used for a half cycle CV. Fig. 5.2 illustrates various possible cycles.

The electrochemical reaction of interest takes place at the working electrode (WE). Electrical current at the WE due to electron transfer is termed as

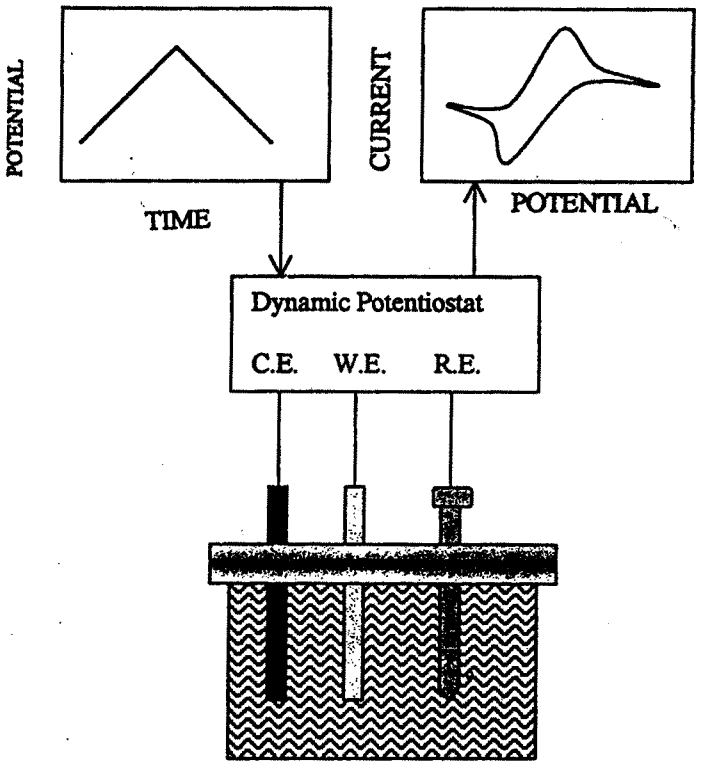


Fig. 5.1 Overall view of the CV experiment.

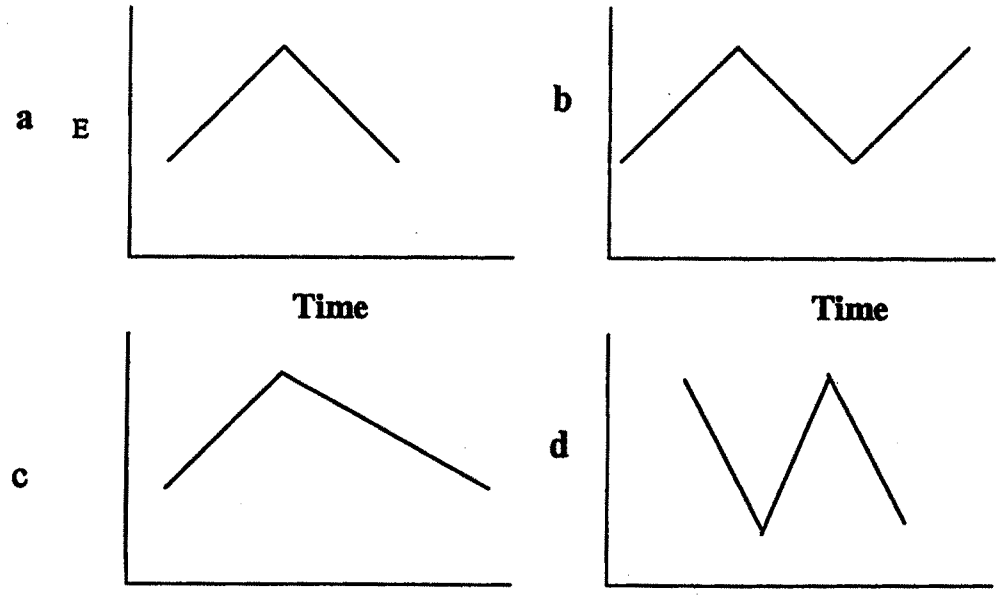


Fig. 5.2 CV waveforms.

'faradaic current'. An auxillary or counter electrode (CE) is driven by the potentiostatic circuit to balance the faradic process at the WE with an electron transfer of opposite direction (e.g. if reduction takes place at the WE, oxidation takes place at the CE). The process at the CE is of not interest, and in most experiments the small current observed mean that the electrolytic products at the CE have no influence on the processes at the WE. The faradiac current at the WE is transduced to a potential output at a selected sensitivity, expressed in amperes per volt, and recorded in digital or analog form. The CV response is plotted as current versus potential.

In this study a three-electrode EC cell has been used. The configuration of the cell was as follows;

$$FTO/\ Nb_2O_5/\ 0.1\ N\ H_2SO_4\ /C;\ SCE$$

Cyclic voltammetry (CV) was performed for all the annealed samples, NA250 to NA450 in an aqueous proton containing electrolyte, 0.1N $H_2SO_4$ at room temperature. Fig. 5.3 shows CVs of these samples at 50 mV/sec scan rate, which are similar to that reported for conventionally deposited $Nb_2O_5$ [12]. During the potential sweep, the current resulting from ion intercalation and deintercalation was measured. A cathodic scan to the extreme potential of –0.45 V (SCE) caused the films to turn blue and at an anodic scan to + 0.25 V (SCE), the films became almost transparent. If the colour bleach cycles are repeated similar CVs , with no much change in shape and sizes are observed. This evinces that all the annealed samples exhibit electrochromism.

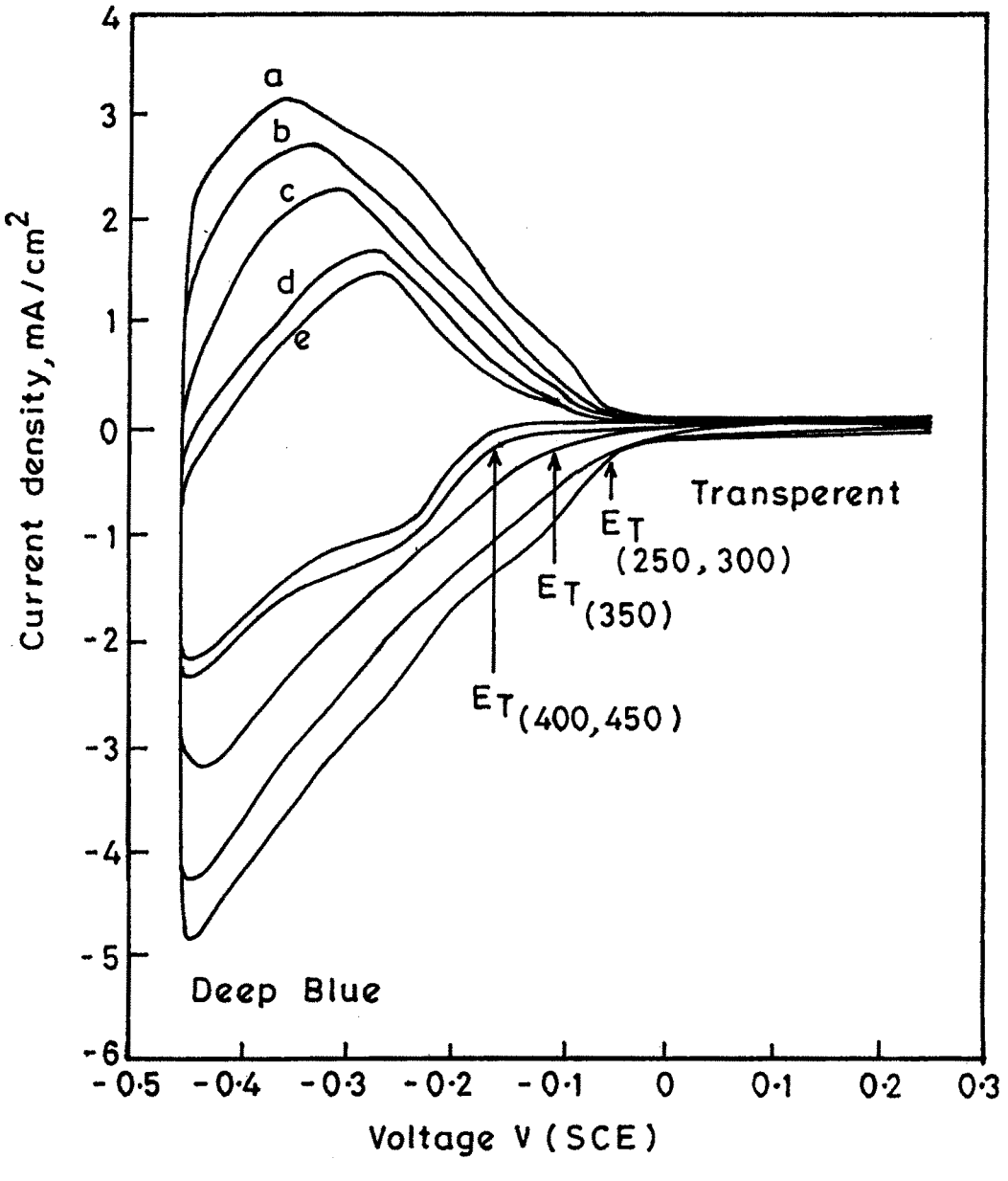


Fig. 5·3 - Cyclic voltammograms for a) NA 250 b) NA 300 c) NA 350 d) NA 400 and e) NA 450 samples at 50 mV / sec scan rate.

The curves show a single oxidation-reduction cycle, with oxidation and reduction peaks. The colouration and bleaching of the $Nb_2O_5$ film is associated with intercalation (insertion) and deintercalation (egress) of $H^+$ ion and electrons in the film according to equation 5.3;

$$Nb_2O_5 + xH^+ + xe^- \rightarrow Hx\,Nb_2O_5 \qquad .....(5.3)$$

(transparent) (blue)

Thus the film can be reversibly made transparent by electrochemical oxidation and coloured by reduction in a proton-containing electrolyte. From Fig.5.3 different parameters associated with ion intercalation and deintercalation of $H^+$ into and out of $Nb_2O_5$ host lattice were calculated and are given in Table 5.1.

The anodic peak potential 'Epa' vary with the sample. For sample NA250 , Epa was lowest (-0.37 V (SCE)). Anodic shift in Epa was observed for samples from NA 250 to NA450. The threshold voltage $E_T$, at which ionic intercalation begins also varies with the samples. For NA250 and NA300 samples it is same, i.e. about –0.05 V (SCE) stating that $H^+$ ion intercalation begins at this potential causing niobium bronze, which renders colouration. This indicates that onset of ionic intrcalation into host lattice depends on crystallinity of the films, for amorphous samples it is high whereas for crystalline samples it is low.

The magnitudes of both the anodic and cathodic peak currents were maximum for sample NA250 among all the samples. This suggests that extent of $H^+$ ion intrcalation as well as deintercalation is maximum for amorphous samples, which wanes for crystalline samples.

**Table 5.1: Different parameters associated with intercalation and deintercalation of $H^+$ ions from $H_2SO_4$ electrolyte into and out of sprayed $Nb_2O_5$ thin film samples**

| Sample | Structure | $E_{pa}$, V(SCE) | $E_T$ V(SCE) | $I_{pa}$, mA | $I_{pc}$, mA | D, $10^{-7}cm^2 S^{-1}$ | $T_c$,S | $T_b$,S | ΔOD | CE $cm^2C^{-1}$ |
|---|---|---|---|---|---|---|---|---|---|---|
| NA250 | M | 0.37 | -0.05 | 3.2 | 4.8 | 1.7 | 12 | 9 | 0.51 | 26 |
| NA300 | M | 0.33 | -0.05 | 2.8 | 4.3 | 1.4 | 12 | 9 | 0.41 | 24 |
| NA350 | M+T | 0.30 | -0.10 | 2.4 | 3.2 | 1.0 | 12 | 6 | 0.33 | 23 |
| NA400 | M+T | 0.28 | -0.17 | 1.8 | 2.3 | 0.93 | 12 | 6 | 0.31 | 23 |
| NA450 | M | 0.27 | -0.17 | 1.6 | 2.1 | 0.78 | 12 | 5 | 0.21 | 19 |

M : Monoclinic; T : Tetragonal, Epa : Anodic peak potential; $E_T$ : Threshold voltage, ipa : Anodic peak current; ipc : Cathodic peak current; D : diffusion coefficient; tc : colouration time; tb : bleaching time and CE : colouration efficiency.

The diffusion constant of $H^+$ ions is calculated from the Randell-Sevcik equation;

$$ip = 2.72 \times 10^5 \times n^{3/2} \times D^{1/2} \times C_O \times \nu^{1/2} \quad .....(5.4)$$

Where D is the diffusion constant, Co is the concentration of active ions in the solution, ν is the scan rate, n is the number of electrons and is assumed to be 1, ip is the peak current density (ipa-anodic peak current density, ipc-cathodic peak current density). The values of ip have been taken from fig.5.3. By substituting all the values, diffusion constants were calculated and are listed in Table 5.1. It is observed that for sample NA250, D is minimum. It is known that large film thickness and a high intercalation level gave minimum diffusion constant. This evokes that sample NA250 has high $H^+$ intercalation level, which decreases with decreasing film thickness i.e. from sample NA300 to NA450.

The diffusion constant is one of the important factor and frequently measured by using various techniques. D was found to lay between $5 \times 10^{-9}$ and $5 \times 10^{-7}$ $cm^2/s$ [24]. It is conceivable that different levels of hydration account for this variation. The values in this study are in good agreement with the reported values.

The voltammetry indicates that $Nb^{5+}$ is reduced to a lower valence state $Nb^{4+}$ by protonation, which returns to the original valency through de-protonation.

**5.2.3.1Chronoamperometry (CA)**

CV is a powerful technique because the CV wave-shape is sensitive to all the parameters of the electrochemical mechanism. For the same reasons, however, a full quantitative analysis with CV can be difficult. It is usually helpful if

qualitative or quantitative information can be obtained from other sources. Potential step methods can play a complimentary role to CV in the analysis of electrochemical mechanism. This is because they can be performed under conditions of a fast and irreversible forward heterogeneous rate constant.

An overview of CA experiment is shown in Fig.5.4. The potential waveform imposed at the WE for the double potential step (DPS) is also shown in Fig.5.4. The characteristic of the waveform are the initial potential Ei, the step potential Es, the step time t and final potential Ef. Here we consider only the case of Es = Ef. Normally electrolysis occurs at the initial potential setting and the potential is stepped to a voltage well beyond the formal reduction potential of the principle electro-active species, that undergoes reduction or oxidation.

In this study chronoamperometry (CA) was used to measure the speed of electrochromic response and to apprehend intercalation and deintercalation mechanisms. To examine chronoamperometric response initially an external voltage of –0.4V (SCE) was applied between $Nb_2O_5$ film and counter electrode and variation in intercalation current (Ji) was monitored with respect to time. Fig.5.5 shows CA response for all the samples. In response to this intercalation, current (Ji) increases rapidly up to its maximum and decays further to a constant value. The colouration time 'tc' (time required for the intercalation current to stabilize at its lowest value) is estimated to be 12 sec. for sample NA250. The

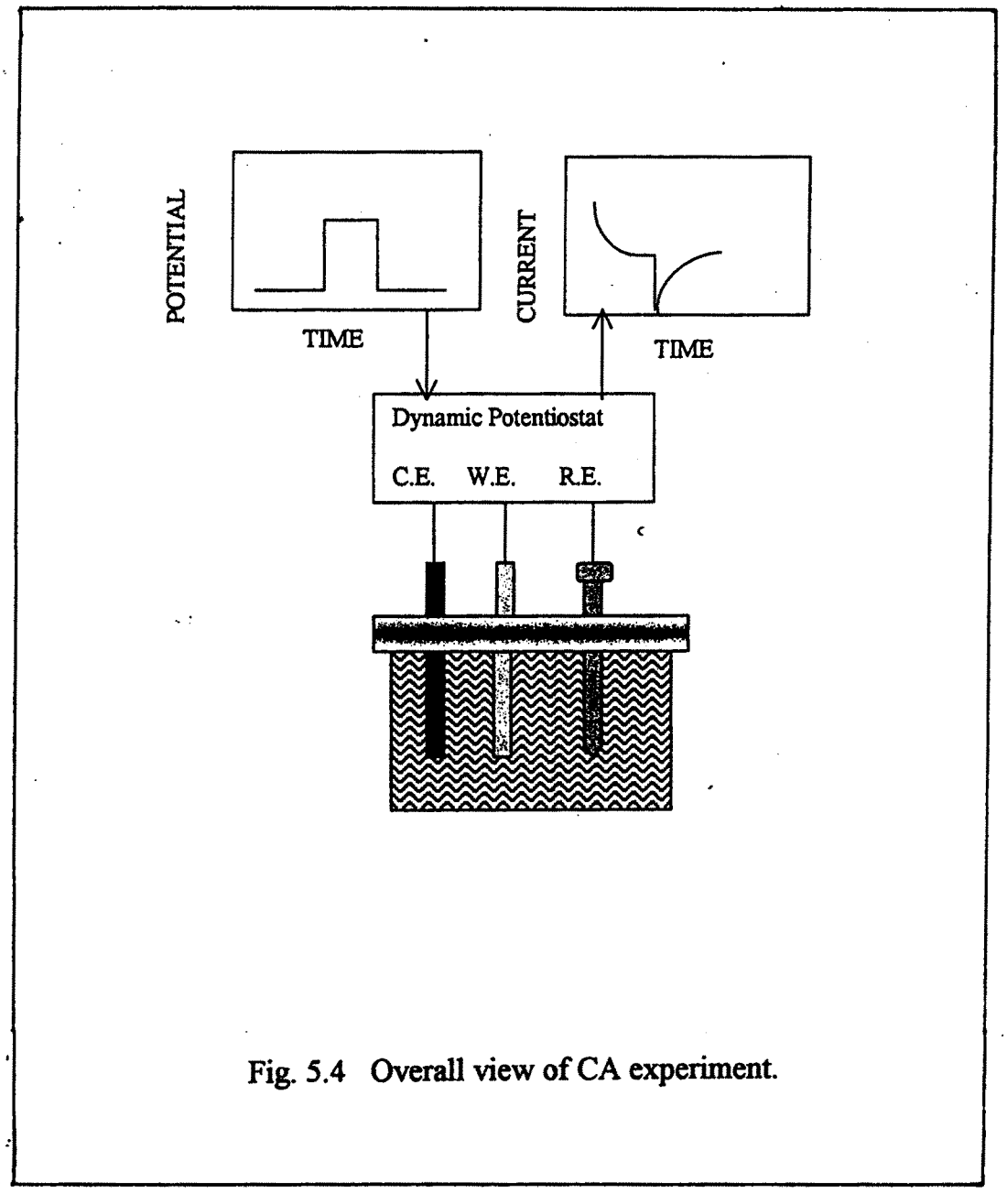


Fig. 5.4 Overall view of CA experiment.

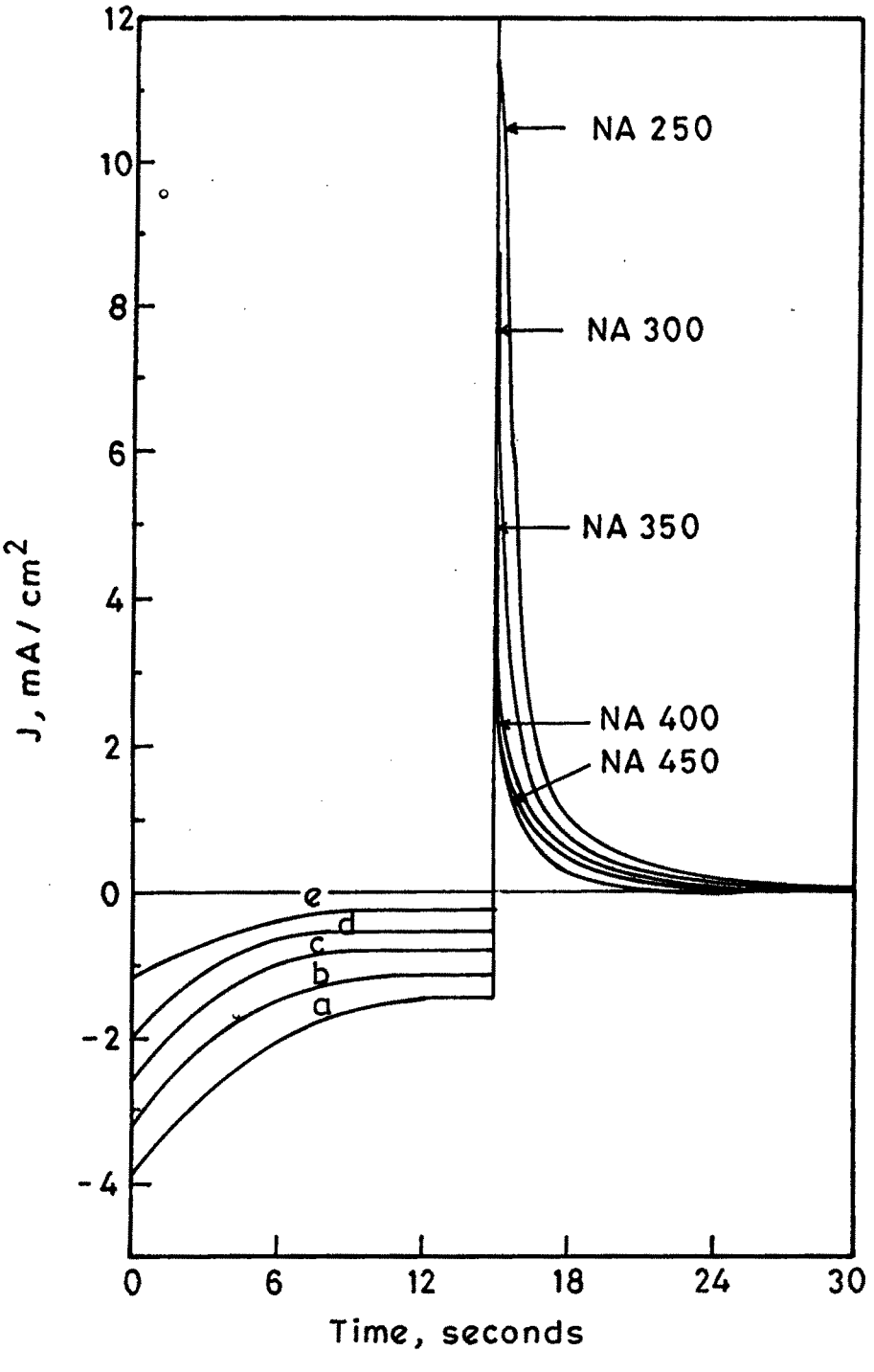


Fig. 5·5 - CA curves of the EC cell formed with a) NA 250 b) NA 300 c) NA 350 d) NA 400 and e) NA 450 samples at Potential ± 0·4 V (SCE).

applied voltage was then switched to + 0.4 V (SCE), which results into rapid increase in deintercalation current followed by sharp decays to a constant value. The bleaching time 'tb' (time required for the deintercalation current to stabilize at its lowest value) is estimated to be 9 sec, for sample NA 250. The values of 'tc' and 'tb' are given in Table 5.1

The asymmetry in current response is typical for materials, which exhibit different conductivity in different oxidation states. The higher bleaching current arises from good conductivity of niobium bronze and rapid decay in current is due to conductor-to-insulator transition. On the other hand insulator to conductor transition has slower transient. Intercalation is largely governed by the properties at the boundary between the electrolyte and the $Nb_2O_5$ film, whereas deintercalation is mainly influenced by ion transport in the film. For asymmetric barrier the time dependence Ji(t) can be obtained from following equation [25].

$$Ji(t) = t^{-1/2} \quad \exp(Ei/RgT) \qquad \text{.....(5.5)}$$

Where Ei is the voltage applied during intercalation process, Ji(t) is intercalation current density, Rg is gas constant, and T is the inverse temperature. Fig.5.6 (a) shows a plot of log Ji versus log t for intercalation, typically for a potential step of ± 0.4 V (SCE). The slope of the intercalation was calculated to be 0.52 (in ideal case it is 0.5) . The discrepancy in the observed and ideal values of slope may be attributed to the ionic diffusion for species intercalated in the film.

Faughnan et al. [26] have shown that, the time dependence Jdi(t) (deintercalation current density) can be obtained by using following equation.

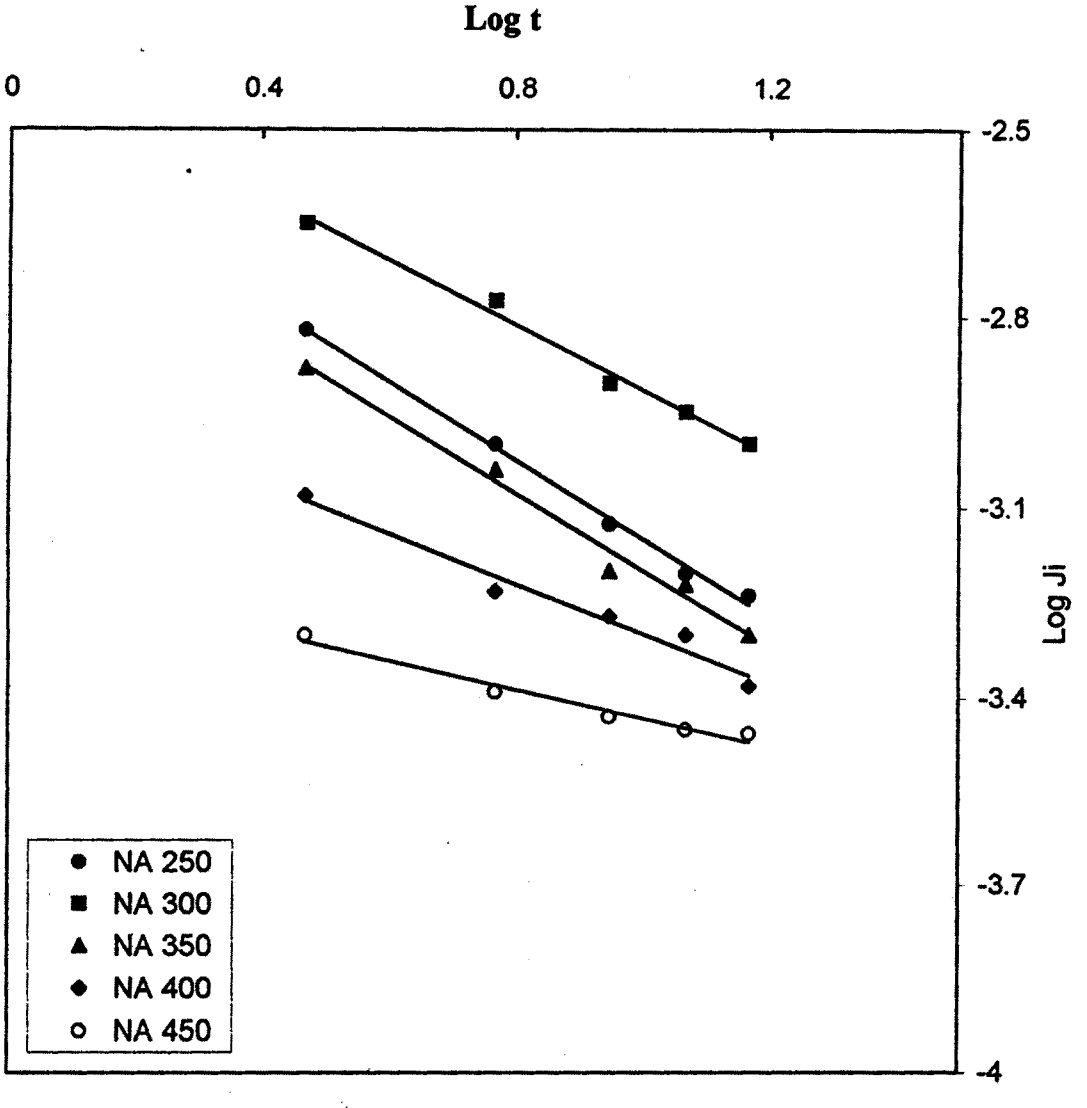


FIG. 5.6 a) Variation of log of intercalation current ($J_i$) versus log of time (t)

$$Jdi(t) \quad \alpha \, Dm^{1/4} \, Ed^{1/2} \, t^{-3/4} \qquad .....(5.6)$$

The slope of log Jdi versus log (t) plot for de-intercalation (Fig.5.6 (b)) was calculated to be 1.8 showing deviation from the theoretical expression for Jdi. Similar results have been reported for tungsten oxide thin films by Nagai and Kamimori [27].

Chronoamperometry was used to study the kinetics of ion intercalation into films made by sputtering followed by oxidation post-treatment [28]. The intercalation current varied with time as $t^{-1/2}$ , which is consistent with a diffusion process. The de-intercalation current was measured for sol-gel prepared films [17], the initial time evolution appeared to lie in between $t^{-1/2}$ and $t^{-3/4}$, where the former dependence accounts for diffusion and the latter is consistent with field driven space-charge limited ion flow.

The cathodic charge densities ($\Delta$ Qi) , resulted from $H^+$ ion intercalation into $Nb_2O_5$, were measured from integration of colouration currents for all the sample. Fig.5.7 shows the $H^+$ charge densities inserted in samples NA250 to NA450. The exchanged charge increases with the thickness of the films and varies from 11 mc/cm$^2$ for NA450 sample to 19 mc/cm$^2$ for NA250 sample.

### 5.3.2 Optical transmittance study

Initially the NA250 sample was coloured (reduced) by applying –0.45 V(SCE) for about 30 seconds, withdrawn from the EC cell and immediately submitted for spectrophotometric measurements. The transmittance spectrum in

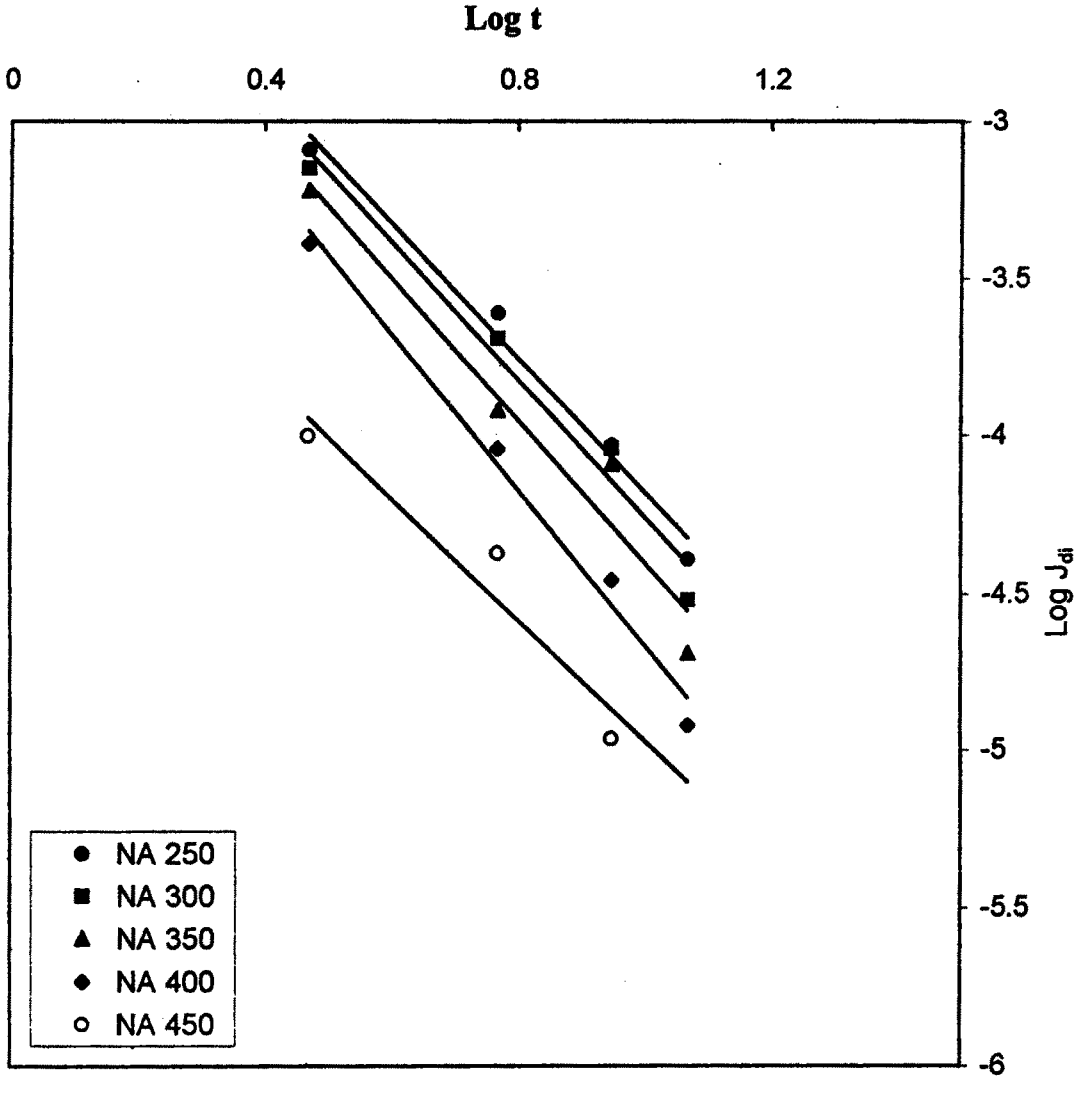


FIG. 5.6 b): Variation of log of deintercalation current ($J_{di}$) versus log of time (t)

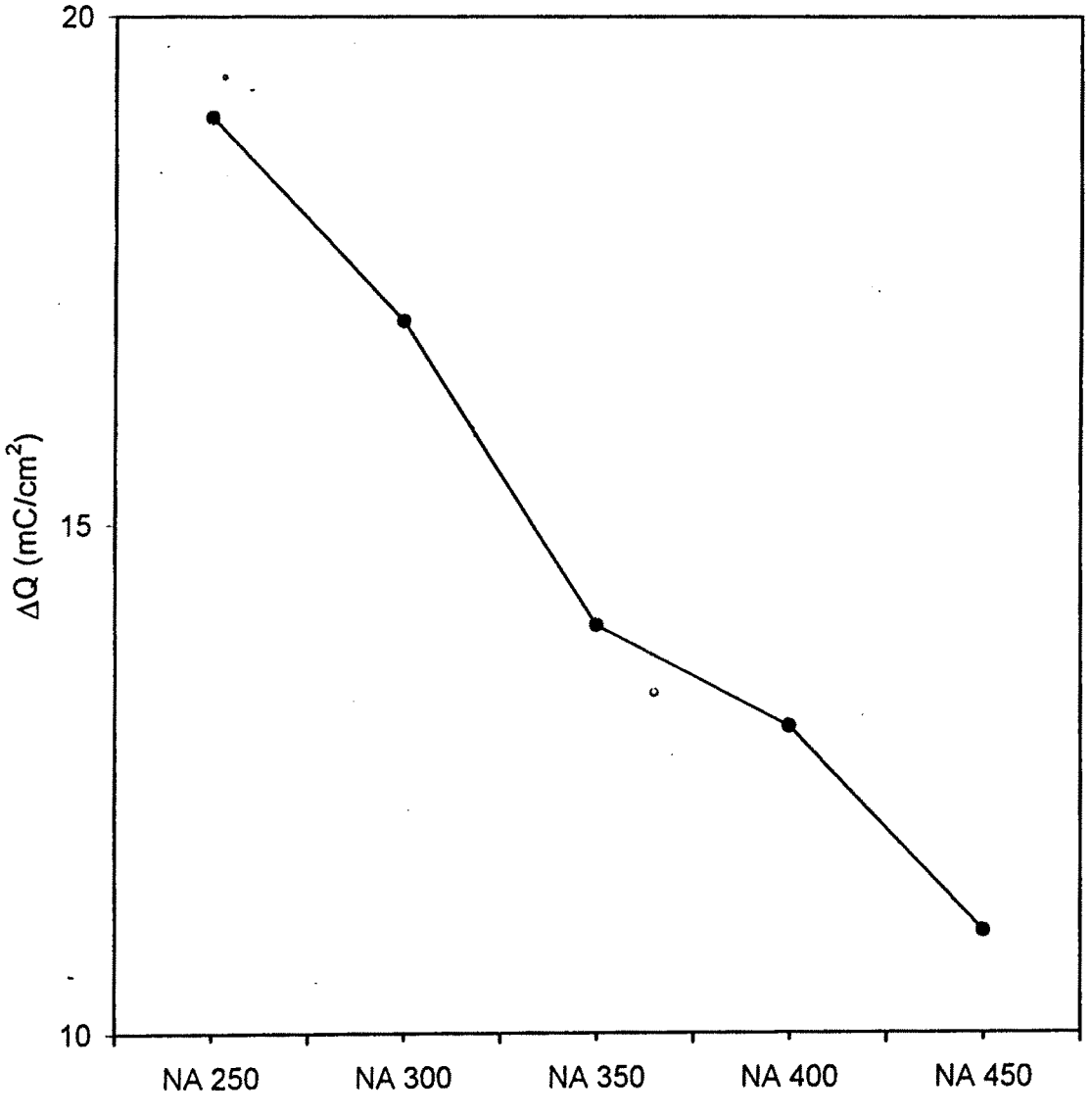


FIG. 5.7: $H^+$ charge densities inserted in samples NA250 to NA 450

the range of wavelength between 350 to 850 nm was recorded. Afterwards the sample was again placed in EC cell and bleached (oxidized) by applying + 0.45 V(SCE).

(SCE) for about 30 seconds, and its transmittance spectrum was recorded. Similar procedure was adopted for all other samples. Fig.5.8 (a-e) shows transmittance spectra for all the samples.

For all the samples it is observed that the insertion of $H^+$ ions changes the transmissivity (due to change in colour to blue) from the near UV up to the near IR range, with a maximum change around 510 nm. For the thickest and amorphous sample NA250 this change ($\Delta$ OD) is maximum. The values of $\Delta$OD are given in Table 5.1.

The colouration efficiency (CE) was calculated using following equation

$$CE = \Delta OD/\Delta Q \qquad .....(5.7)$$

It is an important parameter to probe the potential of a material as an electrochromic material. It is defined as the ratio of optical density ($\Delta$OD) of the film in its coloured state and bleached state at a certain wavelength ( $\lambda$ ) and corresponding injected (or ejected) charge density ($\Delta$Q). The optical density change is obtained by the following equation.

$$\Delta OD(\lambda) = \ln [\, To(\lambda) / Tx(\lambda) \,] \qquad .....(5.8)$$

Where $To(\lambda)$ is the transmittance of the bleached state and $Tx(\lambda)$ is the transmittance of the coloured state at particular wavelength ($\lambda$).

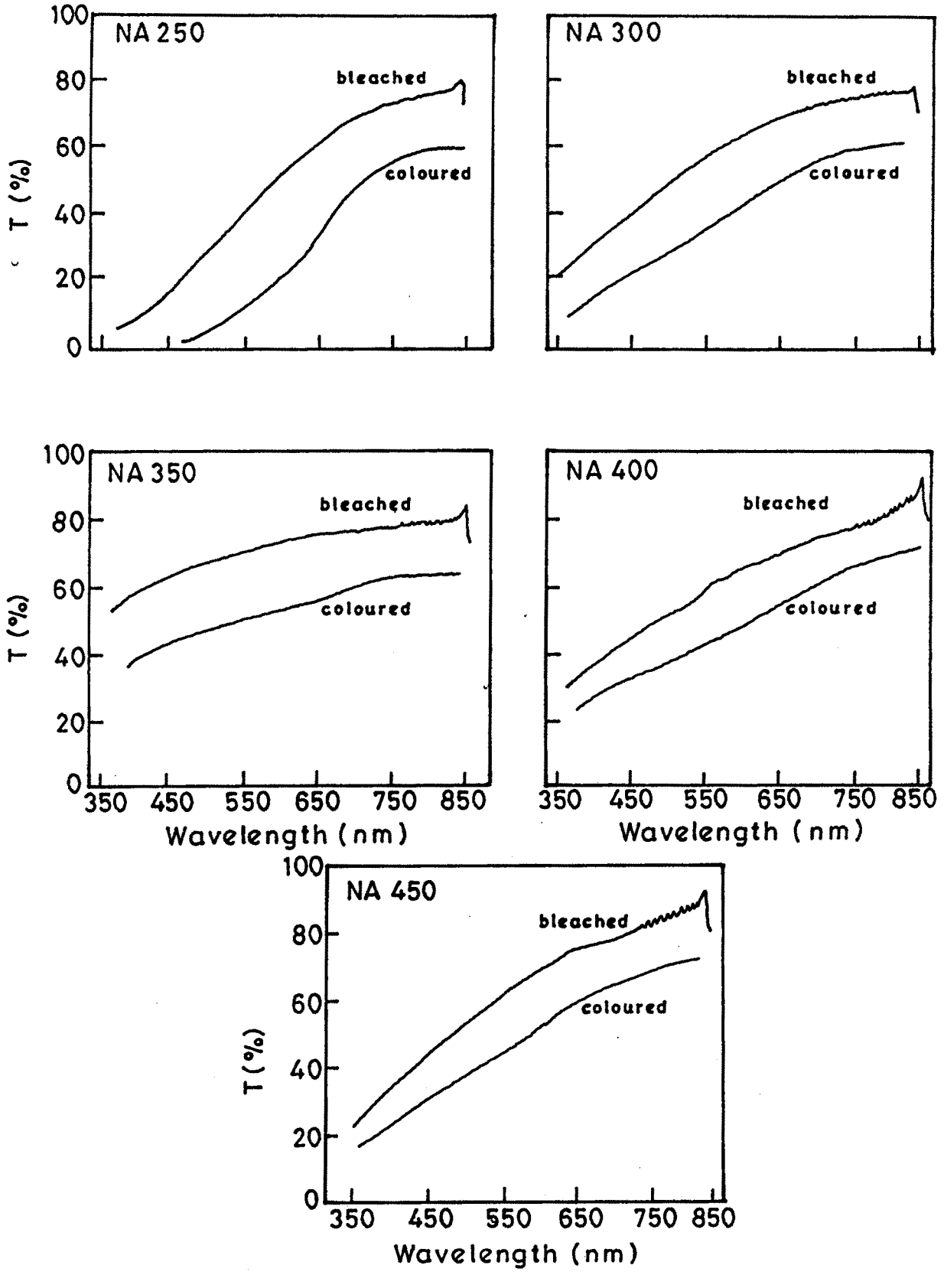


Fig. 5·8 - Plot of optical transmittance against wavelength for coloured and bleached Niobium oxide thin films.

After substituting values of all the parameters the colouration efficiency for all the samples were calculated, and are listed in Table 5.1. Samples NA250 exhibit maximum CE than other samples.

Cogan et al.[28] reported spectral coloration efficiencies for Nb oxide films made by reactive r.f. sputtering in Ar + $O_2$ followed by lithium intercalation, about 34 $cm^2C^{-1}$ at $\lambda$ = 0.6 μm and substrate temperature 310°C. For low substrate temperature about 40°C. The CE was 10 ± 3 $cm^2C^{-1}$. Porous Nb oxide films made by sputtering in $N_2$ followed by oxidation had a CE of 25 to 30 $cm^2C^{-1}$ at $\lambda$ = 0.62 μm [27], whereas a sol-gel produced film had about 6 $cm^2C^{-1}$ at $\lambda$ = 0.8 μm [17]. The values in this study are in good agreement with the reported values.

### 5.3.3 Electrochemical stability

The films (NA250 to NA450) were coloured and bleached (c/b) by applying ± 0.45 V(SCE) for several times in 0.1 N $H_2SO_4$ electrolyte. The insertion (reduction) and extraction (oxidation) processes were found to be stable and fully reversible up to about 1 x $10^3$ c/b cycles, indicating that all the samples have appreciable stability in liquid electrolyte. After these cycles both anodic and cathodic currents starts decreasing rapidly indicating deterioration of the samples.

Both the parameters CE and electrochemical stability are of fundamental importance for eventual industrial development.

## 5.4 Conclusions

Electrochemical behaviour of $Nb_2O_5$ films deposited by spray pyrolysis technique in $H_2SO_4$ electrolyte is almost similar to the films deposited by other conventional techniques. The onset of ionic intercalation into host lattice depends on crystallinity of the films, for amorphous samples it is high where as for crystalline samples it is low. The diffusion constant D was found to lay between $1.7 \times 10^{-7}$ and $0.78 \times 10^{-7}$ $cm^2/s$ for NA250 to NA450 samples. The response time for colouration was about 12 seconds and for bleaching was about 9 seconds. The colouration efficiency was found to lay between 19 and 26 $cm^2\ C^{-1}$, for samples NA450 to NA250. All the films are found to be stable up-to about $1 \times 10^3$ c/b cycles.

**5. 5 References:**

1 Mandelcorn L., editor, Non-stoichiometric compounds (Academic, New York, 1964)

2 Whittingham M.S. and A.J. Jacobson, editors, Intercalation chemistry (Adademic, New York, 1982).

3 Gunter J.R. and H.R. Osswald, Bull.Inst. Chem. Kyoto Univ. 53, 249-255 (1975)

4 Schollhorn R., Angew. Chem., Int. Ed. 19, 983-1003 (1980)

5 Myland J.C. and K.B.Oldham, J.Electroanal. Chem. 347, 49-91 (1993)

6 Kirkup L., J.M.Bell, D.C.Green, G.B. Smith and K.A. Mac Donald, Rev. Sci.Instrum. 63, 2328-2329. (1992)

7 S.K.Deb. Solar Energy Mater. 25 (1992) 327

8 C.G. Granqvist, Solid State Ionics 53-56 (1992) 479

9 C.M. Lampert and C.G. Granqvist in : Large area chromogenics : Material and Devices for Transmittance control (Eds) (SPIE IS 4, C.M.Lampert and C.G. Granqvist, Optical Engineering Press, Bellingham, WA., 1990) P.2

10 R.B.Goldner, F.O. Amtz, G.Berera, T.E.Hass, G.Wei, K.K.Wong and P.C.,Yu. Solid State Ionics 53-56 (1992) 617

11 N.Ozer, T.Barettoi, T. Buyuklimanli and C.,M.Lampert, Sol. Energy Mater. Solcells 36 (1995) 433.

12 C.G.Granqvist Handbook of Inorganic Electrochromic Materials (Elsevier, Amsterdam 1995)

13 R.Cabnel, J.Chaussy, J.Mazuer, G.Delabouglise, J.C. Joubert, G.Barral and C.Montella, J.Electrochem. Soc. 137 (1990) 1444.

14 D.K.Benson and C.E.Tracy, Chemtech. Noivember (1991) 677

15 J.G. Zhang, C.E.Tracy, D.K.Benson and S.K.Deb; J.Mater. Res. 8 (1993) 2649

16 N.Hara. E. Takahashi, J.H. Yoon, and K.Sugimoto, J.Electrochem. Soc. Ionics 141 (1994) 1669

17 G.R.Lee and J.A.Crayston, J.Mater.Chem. 1 (1991) 381

18 B.Reichmann, A.J.Bard, J.Electrochem. Soc. 127 (1980) 241

19 M.A.B.Gomes, L.O.S.Bulhoes, S.C.Castro, A.J.Damiao, J.Electrochem. Soc. 137 (1990) 3067

20 M.C.Alves, M.Sc. thesis, Federal Uni. Of S90 Carlos, Sao Carlos, Brazil (1989)

21 B.Ohtani, K.Iwai, S.Nishimoto, T.Inui, J.Electrochem. Soc. 141 (1994) 2439

22 M.A.Macedo, L.H. Dall Antonia, M.A. Aegerter, in : J.D. Mackenzie (Ed), Proc. Sol-gel optics II, Pv 1758, SPIE, Bellingham, USA, 1992 P.320

23 M.A.Aegerter, in : R.Reisfeld, C.K.Jorgensen (Eds), Structure and Bonding, Vol 85 , Springer, Berlin, 1996

24 Gomes M.A.B. and L.O.de S. Bulhoes, Electrochim. Acta 35, 765-768 (1990)

25 R.S.Crandall and B.W.Faughnan, Appl.Phys. Lett., 28 (1976) 95

26 B.W.Faughnan, R.S.Crandall and M.A.Lampert, Appl.Phys. Lett., 27 (1975) 275.

27 J.Nagai and T.Kamimori, Jap. J.Appl.Phys., 22 (1983) 681

28 Cabanel R., J.Chaussy, J.Mazuer, G. Delabouglise, J.C. Joubert, G.Barral and C.Montella, J.Electrochem. Soc. 137, 1444-1451 (1990) Repeated 13

29 Cogan S.F., E.J. Anderson, T.D.Plante and R.D.Rauh, Proc.Soc. Photo-opt. Instrum. Engr. 1016, 57-62 (1988).